

Magnetic Resonance Elastography in Bounded Media

A. Kolipaka¹, K. P. McGee¹, A. Manduca¹, K. J. Glaser¹, P. A. Araoz¹, and R. L. Ehman¹

¹Department of Radiology, Mayo Clinic, Rochester, Minnesota, United States

Introduction:

Magnetic resonance elastography (MRE) [1] is a noninvasive phase-contrast technique for spatially resolving the shear modulus μ of tissue like materials. Current methods for calculating μ ignore geometric considerations by locally assuming a uniform, infinite medium [2]. The purpose of this work is to validate two new MRE-based methods for estimating μ in objects in which geometric effects dominate.

Theory: MRE-based estimation of shear modulus for two geometric shapes were considered and included; a beam and spherical shell. The equation of motion of a propagating wave in a beam is given by Eq.1 [3], where I =moment of inertia, E =Young's modulus of the material, w =displacements along the transverse direction, S =cross-sectional area of beam, ρ =density of the material and ω =rotational frequency. E in Eq.1 is converted to shear modulus μ using the relationship $E/2(1+\nu)$, where ν =Poisson's ratio. For a spherical shell the equation of motion is defined by applying Hamilton's variational principle and assuming that radius is greater than thickness of the shell and negligible torsional motion [4].

Methods: All imaging was performed in a 1.5 Tesla MRI scanner (Signa, GE Health Care, Milwaukee, WI) with a standard gradient-recalled-echo (GRE) MRE sequence. **Beams:** Three beams of diameters 2.25 cm, 2.5 cm, and 3.7 cm and lengths of 16.3 cm, 16.7 cm, and 18.5 cm, respectively, and Poisson's ratio of 0.49 were constructed with silicone rubber (Wirosil, BEGO, Germany). The beams were supported and fixed at the ends and an electromechanical driver was placed in contact with the center of the beam to generate vibrations. Data acquisition was performed on the three beams at three different frequencies of excitation: 200 Hz, 250 Hz, and 300 Hz. Additional imaging parameters included TE/TR: 28.6/150 ms, slice thickness: 10 mm, FOV: 18 cm for the 2.25-cm and 2.5-cm beams, 20 cm for the 3.7-cm beam, acquisition matrix: 256x64, α : 30°. The MRE-encoded transverse component of displacement was input to Eq.1 to determine μ . Savitzky-Golay filters [5] were used to provide estimates of the high-order spatial derivatives. **Finite element modeling:** 3D FEM was performed to validate inversion algorithm in beams by comparing stiffness estimates from FEM to those from MRE experiments. All FEM was performed using COMSOL (3.4v, COMSOL AB, Stockholm, Sweden). A frequency response analysis was performed on beams with dimensions matching those of the beams used in the MRE study assuming a homogeneous, isotropic material with Poisson's ratio of 0.49, density of 1000 kg/m³, and shear modulus of 143 kPa. The transverse component of motion was then provided as input to Eq.1 for obtaining stiffness estimates using the MRE inversion. **Spherical Shell:** An ex vivo porcine heart was used as a spherical shell model. A balloon was inserted into the LV of the heart and inflated to static pressures ranging from 58-150 mmHg as shown in figure 1 (a). An in-line pressure transducer was used to record pressure. **Acquisition and Analysis:** A midventricular short axis slice of the porcine heart was obtained at each static pressure with external motion of 200 Hz being applied using a pneumatic driver system. Imaging parameters included TE/TR: 15.7/100 ms, FOV: 8 cm, α : 30°, slice thickness: 10 mm, 256x256 acquisition matrix, and 4 MRE phase offsets. MRE-encoded vertical and horizontal components of motion were converted to radial and circumferential components. These polar components of motion were then input into a thin spherical shell inversion [4] to obtain the effective mean shear stiffness at each static pressure. MR magnitude images from the MRE experiments at each pressure were used to determine the wall and chamber volumes used in a P-V model [4] for estimating the shear stiffness. A least squares linear regression fit to both static MRE and P-V model vs inflation pressure data were also calculated.

Results: Figure 2(a-f) shows the transverse component of displacement obtained from FEM and MRE, and the corresponding stiffness maps obtained using Eq.1 and using a phase gradient (PG) based MRE inversion algorithm, respectively. The mean MRE stiffness values obtained from the region of interest shown in black using Eq.1 and PG were 145.9±24 and 91.3±31 respectively. The results for the FEM were 145.2±16 using Eq.1 and 84.1±7 using PG. Figure 2(g) shows the stiffness values obtained from the MRE experimental data and the FEM simulation data for different sized beams at different frequencies inverted using Eq. 1 and the PG method. Figure 1 (b-e) shows, respectively, a magnitude image with contours delineating the LV myocardium, the radial and circumferential components of motion for one phase offset, and the corresponding stiffness map at a pressure of 150 mmHg. A mean stiffness of 44.7±8.5 kPa was obtained from the region of interest (ROI) shown in white in figure 1(e). Figure 3 shows the linear correlation ($R^2 = 0.99$) between MRE stiffness estimates and pressure. $R^2 = 0.98$ was calculated for the P-V model stiffness versus inflation pressure.

Discussion: The results indicate that MRE inversions that include boundary effects are required for accurate estimation of stiffness. $R^2 > 0.98$ between the stiffness estimates from MRE and the P-V model versus pressure indicate a strong correlation between the two techniques.

References: 1. Muthupillai, R, et al, Science 1995;269:1854–1857. 2. Manduca, A, et al, Medical Image Analysis 2001; 5, 237-254.

3. Junger M,C, et al. Sound, Structures and Their interaction,1972,195-253. 4. Kolipaka, A, et al, In: Proc.16th Annual Meeting of ISMRM, 2008 (p.1031). 5. Press, W.H, et al, Numerical Recipes in C,1992,650-655.

$$EI \left(\frac{\partial^4 w}{\partial x^4} \right) = \rho S \omega^2 w \quad (1)$$

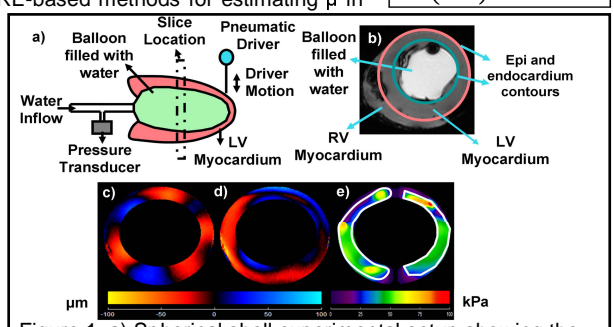


Figure 1: a) Spherical shell experimental setup showing the water-filled balloon, pressure transducer, driver, and imaging slice (b) short axis magnitude image with contours identifying myocardium (c-e) Radial and circumferential components of displacement and the corresponding stiffness map.

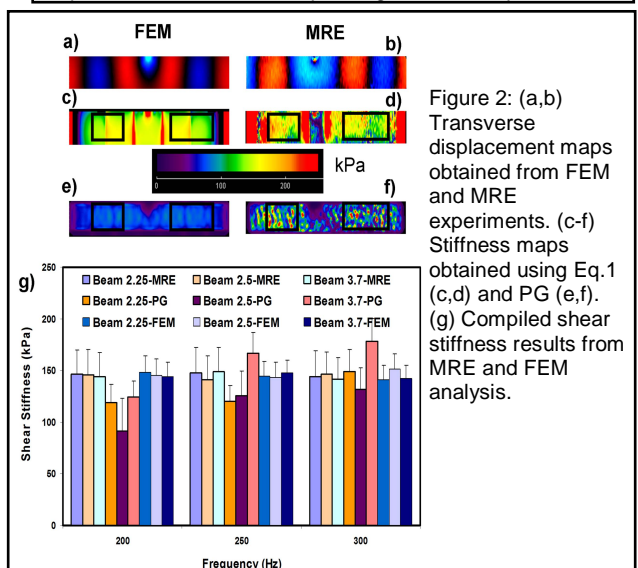


Figure 2: (a,b) Transverse displacement maps obtained from FEM and MRE experiments. (c-f) Stiffness maps obtained using Eq.1 (c,d) and PG (e,f). (g) Compiled shear stiffness results from MRE and FEM analysis.

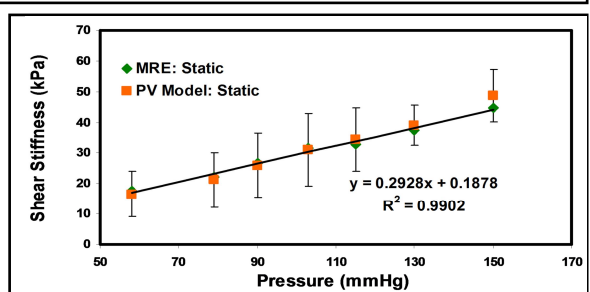


Figure 3: Stiffness vs pressure for both MRE and P-V model.